Ann. Rev. Phys. Chem. 1986. 37 : 493–524

STIMULATED EMISSION PUMPING: New Methods in Spectroscopy and Molecular Dynamics

Charles E. Hamilton, James L. Kinsey, and Robert W. Field

Department of Chemistry and George R. Harrison Spectroscopy Laboratory, Massachusetts Institute of Technology, Cambridge, Massachusetts 02139

INTRODUCTION

Every introductory course in molecular spectroscopy treats the process of assigning spectra as trivial or automatic. At chemically significant levels of vibrational excitation, spectral assignment is certainly not trivial. In fact, the inference of molecular structure from a spectrum may become intrinsically impossible. We deal in this article with spectra far from the textbook limit of small amplitude motions and ask questions of these spectra that are not the traditional ones of equilibrium structure. The task would have been impossible without a technique that offers maximum spectral simplification.

In conventional absorption or emission spectroscopy, transitions emanate from a large number of states; thus, the spectra tend to be quite congested and tedious to assign. One is often limited to investigating the low energy region of a particular potential energy surface, usually because this is the only region where transitions are sufficiently strong and the spectra still remain sufficiently free of congestion to be interpretable. The topic of this review, Stimulated Emission Pumping (SEP), is a new technique for studying an extraordinarily wide range of rotation-vibration levels in the ground electronic states or other low-lying electronic states of diatomic and small polyatomic molecules. The literature has been covered up to January 1, 1986.

SEP is a folded variant of optical-optical double resonance (OODR),

0066-426X/86/1101-0493$02.00

with the identical capabilities of sub-Doppler resolution, state selectivity, and spectral simplification. The transitions involved in SEP are shown schematically in Figure 1. Here, a PUMP laser excites molecules out of a low lying level, usually the vibrationless level of the ground electronic state, to a specific rotation-vibration level in an excited electronic state. A DUMP laser subsequently drives some of the electronically excited molecules back down to an excited vibrational level of the electronic ground state via stimulated emission. In SEP, stimulated emission competes with spontaneous fluorescence when the DUMP laser is tuned onto a linked downward transition. Thus, an SEP spectrum is usually obtained by setting the PUMP laser onto a selected transition and monitoring the decrease in the intensity of undispersed spontaneous fluorescence as the DUMP laser is scanned over various transitions out of the PUMP-selected intermediate level. This decrease in side fluorescence owes to an increase in stimulated emission propagating in the direction of the DUMP beam. Other detection schemes utilizing transient gain (1) or transient optical rotatory power (2, 3) or a dip in multiphoton ionization (4) have also been employed. Other techniques also exist, such as stimulated Raman spectroscopy (5–7), that bear a close resemblance to SEP.

The advantages of the SEP techniques stem mainly from use of a single rotation-vibration level of an *excited electronic state* as the intermediate level. As with other OODR methods, this produces an immediate benefit

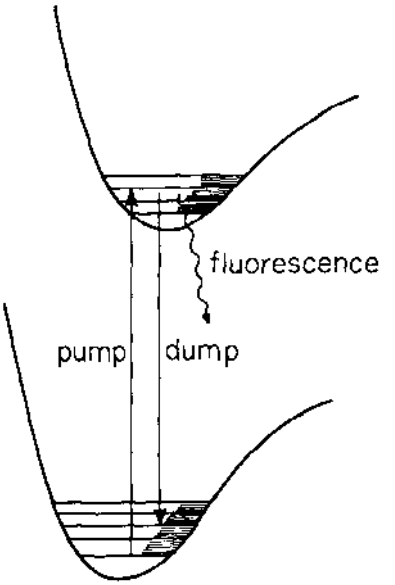

Figure 1 Transitions involved in stimulated emission pumping. The PUMP laser excites molecules to an excited electronic state. The molecules are stimulated down to higher lying levels of the ground state by a DUMP pulse.

by combining rotational-state selection rules for the PUMP and DUMP transitions to eliminate rotational congestion. In the most general case, only three values will be possible for the rotational angular momentum (J) of the final state, and the correct decision among the small number of assignment possibilities is often made without difficulty.

An equally important advantage follows from the vibrational mode selectivity that is achievable with SEP. The range of final vibrational levels reached is determined by the distribution of appreciable oscillator strengths for vibrational transitions between the intermediate and final electronic states. If, as is usually the case, there is a large difference in equilibrium geometry between the ground electronic state and the intermediate electronic state, the Franck-Condon principle will result in significant spreading of the oscillator strength in the small number of vibrational modes that reflect this change in geometry. Consequently, the range of accessible final levels can extend from the vibrationless level upward to very highly excited levels (1.0–3.5 eV). In a polyatomic molecule, this large energetic range can also correspond to changes in the vibrational density of states by several orders of magnitude. Since one major focus of SEP studies is the inference of dynamical behavior of nonstationary states from the collective spectroscopic properties of many stationary states, a wide range of state densities translates into a wide range of time scales over which dynamic behavior may be probed. Other methods that have succeeded in exciting molecules into high energy regions are direct overtone excitation (8) and multiphoton absorption (9). The former has disadvantages arising from the extreme weakness of the overtone transitions as higher levels of excitation are reached and from spectral congestion owing to the absence of rotational selectivity within the thermal distribution of initial states. Likewise, multiphoton excitation suffers from rotational congestion as well as from the existence of distributions in the number of photons absorbed and in the multiplicity of pathways through various intermediate levels.

In principle the spread-out Franck-Condon intensity distribution could also be taken advantage of in resolved fluorescence from the same intermediate level as that used in SEP. The advantage of SEP is that it forces all of the signal into a single resolution element, whereas resolved fluorescence is passive and only a tiny fraction of the emission signal falls on the spectrometer exit slit. The requirements for high resolution, especially in regions of high vibrational density, make resolved fluorescence prohibitive at the fluorescence intensities obtained subsequent to pulsed excitation of a single rovibronic level. In SEP, the resolution is determined by the spectral width of the PUMP and DUMP lasers that induce specific transitions.

How have SEP studies taken advantage of the large range of vibrational excitation that is accessible within the electronic ground state? In the lower energy regions, rather conventional spectroscopic goals have been pursued, namely an extension of Dunham-type rotation-vibration analyses (10) and Stark-effect measurements of dipole moments (11). SEP intensity for relatively low-lying states is primarily confined to levels with excitation in modes that accommodate the difference in the equilibrium geometries of the ground and excited electronic states. In a relatively dense manifold of levels, however, the likelihood increases for a near-degeneracy between one of these intensity-carrying "bright" states and one of a different "dark" type, thus giving rise to a spectroscopic "perturbation." In such a case, local deperturbation analysis provides a slight improvement of Dunham-like coefficients for the bright states and a glimpse of a few otherwise unobservable dark states (often assignable only via their perturbation mechanism). Secondary observables such as coupling matrix elements can be obtained for comparison with model predictions. However, local deperturbation cannot reveal large Fermi-type interactions that may seriously compromise any mechanical significance of Dunham constants.

With an increase in energy the regular behavior that permits conventional spectroscopic analyses begins to erode. The growing density of states makes perturbations more common. Vibrational assignment eventually becomes impractically difficult, or maybe even impossible in principle. The small-amplitude concepts that are appropriate at low energies become invalid as a molecule acquires "chemically interesting" amounts of energy (e.g. typical activation energies for chemical reaction). In this regime it is natural to turn to dynamical questions such as intramolecular energy transfer, isomerization, and photodissociation pathways. Dynamics can be probed by SEP even though each SEP transition reaches a single rotation-vibration eigenstate, which has no interesting time-dependent properties and certainly no homogeneous broadening. This is accomplished by realizing that the collective properties of *groups* of eigenstates can reveal the time-dependent behavior for hypothetical nonstationary preparations involving various conceivable initial coherent superpositions of the whole group of states. In SEP, the nature of this initial preparation is imposed by Franck-Condon overlap with the "well-behaved" rotation-vibration eigenfunction for the *intermediate* level in the PUMP/DUMP sequence. This is in marked contrast to high overtone excitation (8, 12, 13), which picks out local mode features that have significant oscillator strengths with the *initial* state.

The kinds of experimental inquiries possible through SEP intersect areas of current theoretical activity. In particular, ideas regarding chaotic or ergodic behavior in quantum mechanical systems are the focus of lively

activity (14–19). Many extremely basic questions remain arguable. The aims of experimental SEP studies are quite different from the theoretical ones, though there are connections. It is unlikely that measurements, with all their limitations, can contribute much toward resolving the most gripping philosophical and mathematical issues at the center of the quantum chaos industry. Instead, one is interested in such practical questions as whether there exists a clearcut transition between "regular" and "ergodic" behavior. Such a transition is generally agreed to occur when some crucial density of states is reached. In a small polyatomic molecule, we can hope to go through the crucial region sufficiently slowly to observe the transitional behavior in some detail.

One is interested in whether or not there exist special preparations (stationary or nonstationary) that have built-in "chemically relevant" properties such as bond-specific reactivity. If so, how long do the special properties exist? Are they affected by collisions? Can neighboring eigenstates exhibit striking differences or do all the levels in a given energy range have nearly identical properties (with respect to collisions, external fields, etc)? The spectrum of rotation-vibration levels, as simplified by SEP, can be used to address such questions. The spacings of levels relative to each other, the intensity patterns among them, their collisional properties, their Stark and Zeeman effects, all provide insights.

Bringing these insights into focus is only in its beginning but certain askable and answerable questions have been posed: What fraction of available phase space is actually covered by a given initial preparation? Are there any conserved or approximately conserved observables other than those generated by symmetry (parity, total angular momentum, permutation of identical nuclei)? How long does it take the system to explore uniformly whatever region of phase space it has access to? Does this time depend on details of the initial preparation? Are there "vague tori" on which the classical motion of the system is approximately confined for reasonably long times (19, 21, 22) (e.g. several vibrational periods)? SEP investigations possibly may provide data on real molecules that can be used to address some of these questions. The questions that can be addressed must also reflect the deficiencies of the experiment, such as finite dynamic range and resolution, as well as difficulties in comparing relative frequencies for features separated by more than the range covered in a single high resolution scan of the DUMP laser ($\sim 20\ cm^{-1}$).

In addition to these ideas on ergodicity, our review covers other areas of study utilizing the SEP technique. First we describe SEP spectroscopic studies of formaldehyde. The emphasis here is on the details of the SEP technique and how SEP is used to make precise measurements of vibrational frequencies and anharmonicities of formaldehyde. Most of the

review deals with SEP investigations of dynamical processes in molecules. A discussion is given on how SEP is used to address experimentally many of the questions of quantum ergodicity posed above. The molecule on which these studies are carried out is acetylene, and evidence is presented that supports the existence of quantum ergodicity in high energy regimes. We then discuss a topic closely related to the ideas of ergodicity and quasiperiodicity, namely intramolecular vibrational randomization (IVR). We present results of SEP spectroscopy on formaldehyde that demonstrate how Coriolis interactions bring about IVR, and they are discussed within the context of their implications regarding unimolecular processes, multiphoton excitation, and mode selective excitation. We end with a discussion of a PUMP-PROBE experiment where SEP is used to populate a specific state and a third PROBE laser monitors the time evolution of the prepared state or one of its neighbors. Emphasis is on vibrational and rotational relaxation measurements in *p*-difluorobenzene and on recent measurements of collisional relaxation rates in formaldehyde, where a newly developed polarization probe technique is employed.

SEP SPECTROSCOPIC STUDIES OF FORMALDEHYDE

Many of the earlier SEP studies were spectroscopic investigations of formaldehyde, in which molecular constants were extended and verified for the electronic ground state (10). Since the SEP technique was being refined in much of this work, the discussion that follows covers not only the results of these studies but also how the SEP technique works and some necessary precautions.

The first step of SEP is excitation of a molecule to a single rotation-vibration level in an excited electronic state. Subsequently, the molecule is stimulated to undergo a transition from that level to an excited rotation-vibration level of the ground electronic state. The excited electronic state that serves as the intermediate in formaldehyde is the $\tilde{A}\ ^1A_2$ state (23). The $\tilde{A}$-state has an out-of-plane bent structure, and it is excited via a π^*-n transition. Consequently, the vibrational modes in the $\tilde{X}$-state that are most easily reached by the DUMP step are the out-of-plane bend (ν_4) and the C–O stretch (ν_2). In all of the formaldehyde studies covered in this review, the 4^1 vibrational level of the $\tilde{A}$-state serves as the intermediate level from which all DUMP transitions emanate. The 4^1 level is excited by tuning the PUMP laser to a previously assigned rotational transition in the $\tilde{A}$-$\tilde{X}$ 4_0^1 band.

Most difficulties with SEP are associated with the DUMP transition. All of the SEP experiments are carried out in static gas cells with pulsed

PUMP and DUMP lasers ($\tau \sim 5$ ns, ~ 0.03 cm^{-1} linewidth). The gas cells are arranged in a dual-beam null detection scheme consisting of a REFERENCE side (through which only the PUMP laser passes) and a SIGNAL side (through which both the PUMP and the DUMP lasers pass). The PUMP laser induces fluorescence in both SIGNAL and REFERENCE regions, and a null is obtained in the absence of a DUMP laser resonance. This eliminates most of the effects arising from pulse-to-pulse variations in the intensity, frequency, or spatial profile of the PUMP laser. The null is destroyed when the DUMP laser is present and tuned onto a linked transition because the quantum yield for spontaneous side fluorescence is reduced in the SIGNAL region. The detected SEP signal is the difference in fluorescence levels between the REFERENCE and SIGNAL sides. One must verify that the DUMP laser actually stimulates downward rather than upward transitions (24). This is checked by tuning the PUMP laser to various adjacent rotational levels and determining from the combination differences that the SEP spectra from these levels have assignments consistent with downward rather than upward transitions. For instance, in the formaldehyde study, the PUMP laser is tuned to excite the $J_{0,}$

The J-dependence of the resonant DUMP frequencies from these $J_{0,}$ rotational levels then allows computation of rotational term values in the vibronic level reached by the DUMP transitions under the assumption that the DUMP transitions are downward. If this assumption is incorrect, the calculated term values will decrease rather than increase with increasing J. The real strengths of SEP derive from the combined rotational selection rules for the PUMP and DUMP transitions. It is through these combined selection rules that one is able to make proper line assignments with relative ease. For instance, in the formaldehyde work only $K_a' = 0$ levels are produced by the PUMP laser; thus, the DUMP transitions can access only $K_a'' = 1$ levels (b, c-dipole transitions) or $K_a'' = 0$ levels (a-dipole transitions). From the distinctive patterns of P, Q, R lines that appear when the DUMP laser is tuned onto a, b, or c dipole transitions, the vibrational symmetry species of the $\tilde{X}$-state vibrational level reached is unambiguously determined. This usually leads to an unambiguous vibrational assignment. Figure 2 gives an example in which the PUMP laser is tuned to access the $1_{0,1}$ $2_{0,2}$ asymmetric rotor levels in the $\tilde{A}$-state. DUMP transitions from these levels to the 8530 cm^{-1} region of the $\tilde{X}$-state show an a-type band and three b-type bands. These bands are assigned to the $2_2 4_2 5_1$ and (2_5, $1_1 2_2 4_2$, $3_1 4_4 6_2$) vibrational levels, respectively, since these are the only levels that are consistent with vibrational symmetries determined from a rotational analysis and estimated vibrational energies.

The fact that a given DUMP transition originates from a *single* rotation-

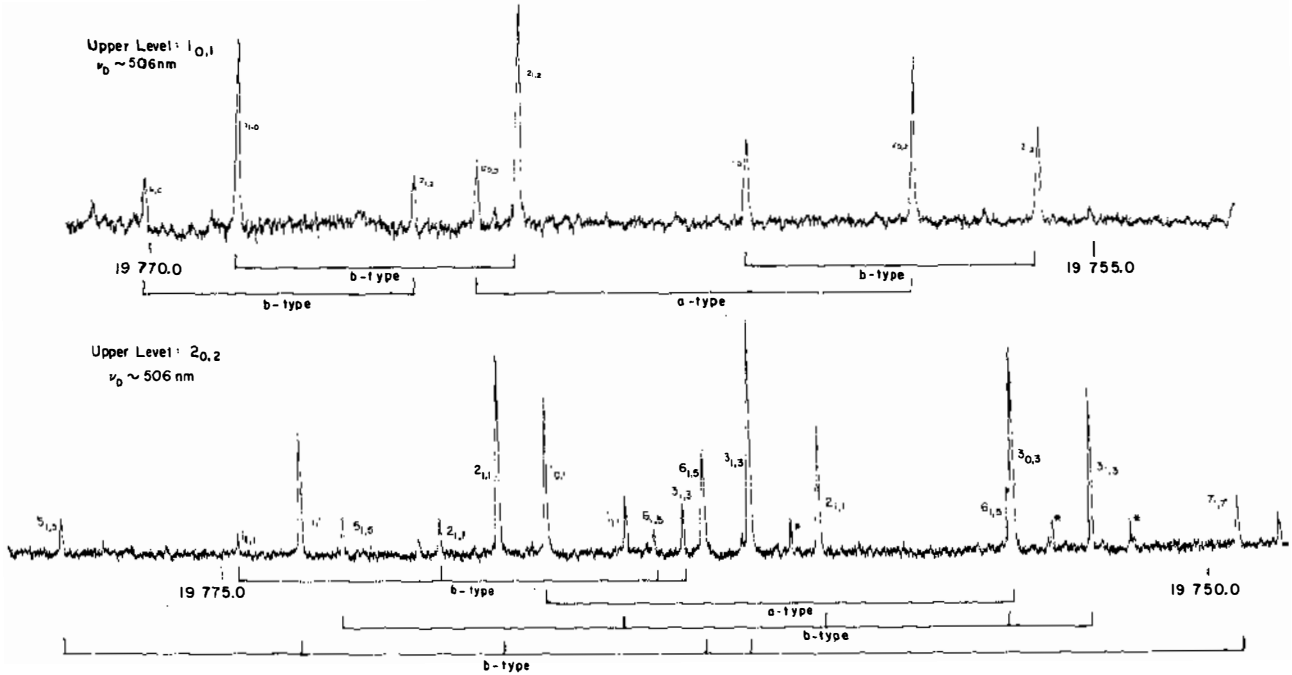

Figure 2 SEP spectra of formaldehyde at ground state energies near 8530 cm^{-1}. The spectra from the $1_{0,1}$ and $2_{0,2}$ intermediate levels lead to unambiguous assignment of the three *b*-type bands as $2_5^0 4_0^1$, $1_1^0 2_2^0 4_2^1$, and $3_1^0 4_4^1 6_2^0$, respectively, and the one *a*-type band as $2_2^0 4_2^1 5_1^0$.

vibration level of the intermediate electronic state gives rise to the simplicity of a SEP spectrum over that found in typical absorption or resolved fluorescence spectra. However, this spectral simplification is degraded if the intermediate level prepared by the PUMP laser is collisionally relaxed into other nearby levels prior to stimulation by the DUMP pulse. Thus, a delay between the PUMP and DUMP lasers that is short compared to the collisional relaxation time of the intermediate level is crucial. Cross sections for relaxation within the excited electronic state are often quite large. Recent transient gain measurements on the $\tilde{A}$-state of formaldehyde (1) indicate that cross sections for depopulation of the prepared level are on the order of 500–600 $Å^2$ for H_2CO/H_2CO collisions. With such large cross sections, collisional relaxation is circumvented only by carrying out these experiments at sufficiently low pressures and with sufficiently short delays between the PUMP and DUMP pulses. Typical pressures used in the formaldehyde experiments are 50–150 mTorr, giving collisional relaxation times on the order of $\sim$100 ns. Delays of the DUMP pulse following the PUMP pulse are from 0–15 ns. Hence, the initially prepared population remains essentially unrelaxed. The "gate time" for SEP is the duration of the DUMP pulse; hence, it can be quite short. Such gating is more difficult in spontaneous fluorescence measurements, which have a characteristic time given by the upper state's decay rate (radiative or collisional).

Much of the work on formaldehyde has focused on identifying new vibrational levels of the $\tilde{X}$-state and extracting the harmonized vibrational frequencies (ω_i^0) and anharmonicities (x_{ij}) that characterize these levels. In the energy range of the $\tilde{X}$-state covered in this work, 4500–9000 cm^{-1}, there are more than 50 vibrational states. Observed energy eigenvalues from these SEP data and FTIR spectra (25) taken in the 400–8100 cm^{-1} region are used to determine a complete set of vibrational Dunham constants through third-order terms, based entirely on observed energy eigenvalues. Some types of vibrational levels are seen in SEP only through perturbations by nearby intensity-carrying levels; the perturbing levels are of the type 2_n4_m and $1_12_n4_m$. The perturbations can be either of the Fermi-type, which is present in the nonrotating molecule, or Coriolis interactions induced by rotations about the *a*-, *b*-, or *c*-axes (26). For the perturbed levels, a "deperturbation analysis" can yield values of the unperturbed eigenvalues and the perturbation strengths. It is the deperturbed energy values that are used in the Dunham analysis. Hence, Dunham coefficients based on such energies contain uncertainties brought in by the deperturbation analysis. Despite the possible shortcomings of an extended Dunham series as an accurate predictor of energies, it is extremely useful to have a fairly reliable functional form that is capable of extending predictions of level positions into unexplored energy regions. Perhaps more importantly,

the Dunham series is invaluable for calculating accurate vibrational densities of state in higher energy regions.

There are standard expressions for obtaining a power series representation of the force field from a set of Dunham coefficients. As yet, no such conversion has been reported for the set of Dunham coefficients obtained for H_2CO by Reisner et al (10). A different approach, developed by Gerber, Roth & Ratner (27), makes direct use of the observed energy eigenvalues in a polyatomic RKR-type inversion. Their method is a semiclassical treatment based on an approximate separation of the vibrational eigenvalue problem through a self-consistent field (SCF) approach. Gerber et al give an example of their procedure for a linear triatomic model; however, it has still not been applied to H_2CO or any other molecule larger than triatomic.

The large set of observed vibrational term values has found applications in variational calculations of vibrational energy levels for semiempirical or *ab initio* potentials. Following seminal work by Handy & Carter (28), Maessen & Wolfsberg (29) tested two empirical force fields by using a product basis of harmonic oscillator wave functions in each of the six normal modes. The full Watson rotation-vibration Hamiltonian for polyatomic molecules is employed (30). Integrals for the variational calculation are evaluated by Gauss-Hermite quadrature. Energy levels up to $\sim$6000 cm^{-1} above the ground state are reported, most of them with errors of $\sim$20 cm^{-1} or less at energies below 2500 cm^{-1}, growing to errors of $\sim$100 cm^{-1} or less near 6000 cm^{-1}. The worst agreement is for levels with excitation in ν_5 and ν_6 (antisymmetric CH stretch and HCO bend, respectively), a fact the authors attribute to inadequacies of the potential in those modes.

Similarly, Romanowski, Bowman & Harding (31) have reported a large variational calculation based on an *ab initio* surface computed by Harding & Ermler (32). An expansion of the Harding-Ermler potential up to quartic terms in the normal mode coordinates is used as the potential in a full Watson Hamiltonian. Adjustments are made in the quadratic terms to achieve better agreement with the observed fundamental frequencies. Two kinds of basis functions are used in this calculation: an uncoupled anharmonic oscillator (UAO) basis, and a basis derived by a vibrational self-consistent field (SCF) approach (33, 34). They report calculated levels up to $\sim$6000 cm^{-1} that are in better agreement with experiment than those of Maessen & Wolfsberg. Most of their levels agreed to within 20 cm^{-1} over the full energy range, and all but one ($4_2 5_1$) were within 30 cm^{-1} of observed levels.

From the coefficients of various basis functions in their UAO-con-

figuration interaction calculation, Romanowski et al conclude that Fermi coupling strongly mixes the $3_1 6_1$, $2_1 6_1$, and 5_1 levels. Combinations of these levels with excited levels of other modes are also believed to be seriously mixed. Romanowski et al suggest that the mixing may even approach a statistical limit. Experimental evidence, however, suggests that the intensity-carrying states ($2_n 4_m$ and $1_1 2_n 4_m$) are relatively pure to much higher energies. The pattern of observed levels up to ~ 10000 cm^{-1} remains well in agreement with the levels predicted semiquantitatively from the Dunham expansion given by Reisner et al (10). Where unexpected levels are found, they are usually weak and always cluster near a predicted strong level. This observation does not contradict Romanowski et al's conclusions about Fermi mixing among the $3_1 6_1$, $2_1 6_1$, and 5_1 levels. However, the existence of mixed coefficients might also result from a need for curvilinear coordinates to describe some of the vibrational modes, such that no normal-mode basis will result in an "almost pure" description for the excited levels.

SEP STUDIES OF MOLECULAR DYNAMICS

SEP Investigations of Quantum Ergodicity

A dynamical phenomenon that has remained relatively uninvestigated experimentally is that of ergodic or chaotic motion in a molecule. This is primarily because such motion is expected to occur in energy regions that are not easily accessible in fairly small molecules. In large molecules such as benzene, the transition to ergodic behavior may occur in a lower and more easily accessible energy region where the spectra tend to become quasicontinuous. However, an understanding of energy randomization in quantum systems is extremely important in that it is intimately tied to intramolecular energy transfer and important dynamical concepts such as RRKM unimolecular rate theory (14–16). To date, a vast amount of theoretical work has been done on coupled oscillator systems (e.g. the Henon-Heiles potential) (17, 19, 21), and there has been much debate over how classical ideas on chaotic behavior carry over to quantum mechanics. SEP on small molecules is quite useful for experimental studies in this area, since one can slowly tune through energy regions with higher and higher densities of states and closely follow the loss of approximately conserved observables. The unique ability of SEP to reach high energy regions in the electronic ground state permits the experimentalist to shed some light on what is meant by quantum ergodicity and what usefulness the quantum ergodicity concept may have. In this section, we describe SEP investigations of acetylene that are aimed at such questions (35–37). Also

we discuss briefly a similar SEP experiment on HCN, with attention directed toward the particular types of motion that are induced in the SEP experiment.

The success of these SEP investigations rests on the existence of a definition of quantum ergodicity and a set of criteria for determining when a spectrum shows signs of ergodic behavior. One definition takes semiclassical quantization as its point of departure. Fundamental to semiclassical quantization is the idea that motion described by a quasiperiodic trajectory has quantized actions (17, 38, 39). The corresponding wavefunction has a well-defined nodal pattern (i.e. easily discernible nodal hyperplanes) described by a set of good quantum numbers corresponding to the constants of the motion. An ergodic trajectory, however, does not have a full set of quantized actions; that is, the number of conserved observables is fewer than the number of degrees of freedom. The corresponding wavefunction has a nodal pattern that appears to be erratic, and many of the quantum numbers that were good in the quasiperiodic regime are no longer definable in an ergodic regime. The only exceptions concern the rigorously conserved observables of energy, angular momentum, and parity. It is possible that broad features composed of many lines in the spectrum will reflect the short time dynamic persistence of "approximately conserved" actions. In this case, the *features* can be assigned, but the individual eigenstates, which correspond to evolution for a time on the order of $h/2\pi$ times the local density of states, do not show any evidence of initial preparation. In classical mechanical studies, Shirts & Reinhardt (21) have invented the concept of "vague tori" in order to describe such behavior. That is, instead of the motion in phase space being constrained to lie on the surface of a so-called "invariant torus" (as is the case for regular motion), it would be *approximately* confined to the neighborhood of such a torus for a long period of time (several vibrational periods for some of the modes). Then a rather abrupt switch would occur to another approximate torus and so on. On an extremely long time scale, the trajectory for such a system would lose its approximate localization, and it would uniformly fill the available phase space.

One of the ways that spectra of the quasiperiodic (regular) and ergodic (irregular) regions of a potential surface should differ is that a spectrum of a quasiperiodic region can be *assigned in principle*, whereas a spectrum of an ergodic region is *intrinsically unassignable*. From a practical standpoint, deciding whether or not a spectrum is "intrinsically unassignable," as opposed to merely extremely complicated, will be a very difficult task. The spectroscopic simplification of SEP helps, but it may not suffice. A more useful criterion for detecting quantum ergodic behavior in a molecule stems from a definition of quantum ergodicity in which a quantally ergodic

region has multiple and overlapping energy level repulsions (16–18). Various statistical properties of the levels, such as the distribution of nearest neighbor energy level spacings, serve as tests for quantum ergodicity. Berry & Tabor (40) have shown that a system of anharmonic oscillators with quasiperiodic dynamics will produce in the semiclassical limit a set of energy levels that are randomly placed with respect to each other. That is, Poisson statistics will be followed. This yields the prediction of an exponential probability distribution for the separation S between adjacent eigenvalues:

$$P_P = \exp(-S/\bar{S})/\bar{S} \qquad 1.$$

where $\bar{S}$ is the average spacing between levels. In this case, the most probable energy level spacing is zero. In an ergodic regime, however, where all of the energy levels strongly repel each other, one expects a nearest-neighbor spacing distribution that vanishes for $S = 0$. Wigner (41, 42) first suggested a distribution of the following form for this case:

$$P_W = \pi S \exp(-\pi S^2/4\bar{S}^2)/2\bar{S}^2. \qquad 2.$$

In the SEP experiments on acetylene, two energy regions of the ground state potential surface are probed, one centered at approximately 9000 cm^{-1} and the other centered at 27900 cm^{-1}. In each of these regions, the vibrational motions excited are primarily the *trans*-bend (ν_4) and the C–C stretch (ν_2). The intermediate level through which the excited vibrational levels are reached is the 3^3 vibrational level of the $\tilde{A}\ ^1A_u$ electronic state. Acetylene has a *trans*-bent molecular structure in the $\tilde{A}$-state and is a near prolate symmetric top. The intermediate level is excited via a π^*-π transition, with the PUMP laser tuned specifically to the 3_0^3 band (ν_3 = *trans*-bend in the A-state). Since bending motions are being excited, the amount of vibrational angular momentum that an acetylene molecule acquires is limited by the approximate selection rule $K_a' - l'' = \pm 1$ for single photon transitions. Here, l'' is the quantum number for the vibrational angular momentum in the electronic ground state and K_a' is a quantum number referring to the angular momentum projection onto the inertial a-axis in the excited electronic state. Since the PUMP transition originates out of the vibrationless state ($l'' = 0$), the combination of the PUMP and DUMP transitions allows access only to the $l'' = 0, 2$ states of the electronic ground state.

The SEP spectra that are observed in the high and low energy regions of the ground state have dramatically different characters. In the 9000 cm^{-1} energy region, the SEP spectrum is completely assignable. Both $l'' = 0$ and $l'' = 2$ states are observed. There appears to be no breakdown of quantum numbers, suggesting that the molecular motion is quasi-

periodic. The spectra recorded at 27900 cm^{-1}, however, are unlike anything that had been measured previously. Under low resolution conditions, the spectra display a number of broad features that are approximately 1.5 cm^{-1} wide and separated from each other by approximately 10 cm^{-1}. An example of one of these low resolution spectra is shown in Figure 3*a*. At higher resolution, each feature is determined to be a clump of approximately 70 lines, each of which has a laser-limited FWHM of approximately 0.03 cm^{-1}. A high resolution spectrum of one of the clumps is shown in Figure 3*b*.

These clumps display several spectroscopic characteristics, many of which suggest that quantum ergodic behavior exists in the 27900 cm^{-1} energy region. An observation that is unrelated to ergodicity is that when different $\tilde{A}$ state vibrational levels are reached by the PUMP step (3^3 and 3^2 levels), the same clumps appear but at DUMP frequencies that are shifted by the energy difference in the $\tilde{A}$ state vibrational levels. This result merely indicates that the clumps arise from some particular structure of the S_0 levels in this energy region, specifically the sharing of Franck-Condon intensity from the intermediate $\tilde{A}$-state level. The detailed structure of the clumps is explained in terms of coupling between two different

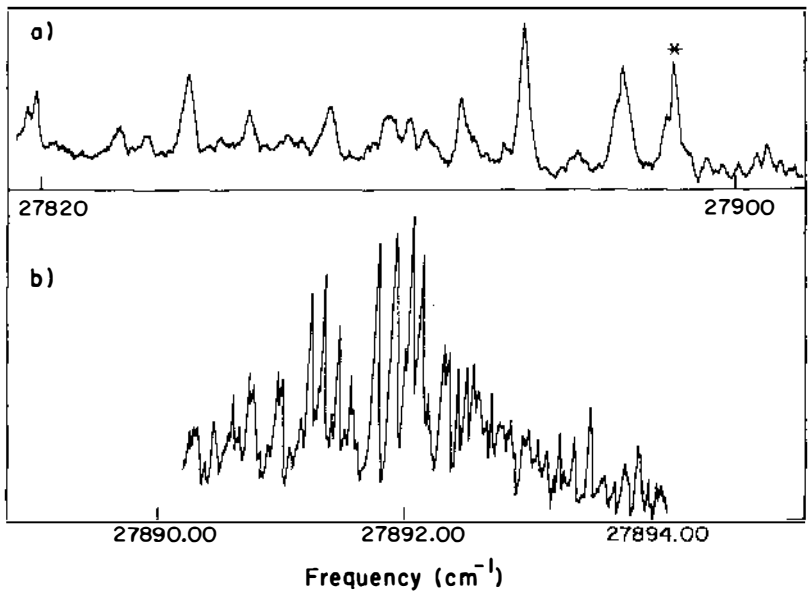

Figure 3 SEP spectra of acetylene near 27900 cm^{-1}. (*a*) Low resolution spectrum in which the 1.5 cm^{-1} features appear. (*b*) High resolution spectrum of the starred feature showing that the feature is a clump of lines.

sets of basis states. One set, referred to as Group I, corresponds to vibrational states with appreciable Franck-Condon overlaps with the 3^3 level of the $\tilde{A}$-state ($v_4 \gg v_2 > v_1$), while the second set, Group II, consists of vibrational states with small overlaps. The density of Group II states is much larger than that of the Group I states ($\rho_{II} \sim 5$ per cm^{-1}; $\rho_I \sim 0.06$ per cm^{-1}), and the high resolution structure of the clumps arises from borrowing of Group I intensity by the Group II states. From a dynamical perspective, the *collection of levels* that make up the clump is the result of a short-time localization on the $\tilde{X}$-state surface, while detailed relationships *among* these levels is indicative of the subsequent dynamical evolution of this initially localized entity.

A revealing characteristic of the clumps is that each clump has a rotational constant associated with it. This property is exhibited in Figure 4, where it is shown that as the PUMP is tuned to excite different J' states within the $\tilde{A}$-state, the energy of center of gravity of a particular clump

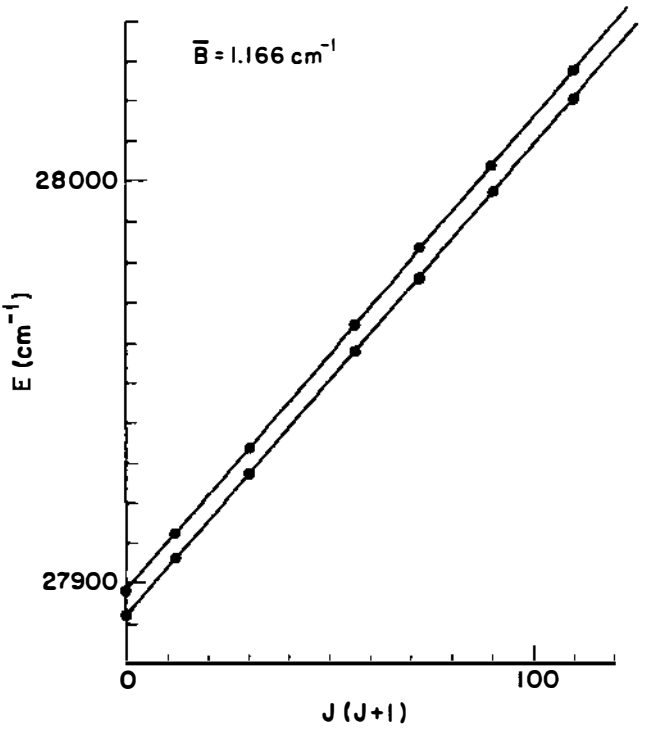

Figure 4 Rotational dependence of two SEP clumps. The linearity of the plot and the existence of $J'' = 0$ clumps indicate that the DUMP laser is accessing only the $l'' = 0$ states. The $l'' = 2$ states have become unobservably weak.

tracks as $E = E^0 + B_{\text{clump}} J'(J'+1)$. This confirms the fact, which is independently established by polarization SEP studies (36), that the DUMP transitions are Q-branch transitions. More importantly, the results show that the short time dynamics samples a localized preparation with a surprisingly large effective B-value. When J'' is lowered to 0 or 1, with $J'' = 0$ being reached by an R-branch DUMP transition instead of the usual Q-branch transitions, the clumps are still observed. Since the vibrational angular momentum l'' can be no larger than J'', only the states with $l'' = 0$ are being observed. Apparently, $l'' = 0$ remains a good quantum number, but $l'' = 2$ has broken down in some way. Presumably, the $l'' = 2$ states have undergone so much mixing with other states that extensive intensity sharing has made these states unobservably weak.

We are now in a position to test whether the $l'' = 0$ states are ergodic or not. This information is contained in the high-resolution structure of the clumps. As stated above, the nearest neighbor level spacings are expected to exhibit different statistical patterns, depending on whether the levels are characteristic of quasiperiodic or ergodic regimes. In the acetylene work, the first three moments of the nearest neighbor spacing distributions are determined for six different clumps. Figure 5 shows the values of the second and third moments for all six clumps as well as expectations based on Poisson and Wigner statistics (*solid lines*). Due to the finite resolution of the SEP experiments, the expected results for the Poisson and Wigner distributions are calculated for various values of the ratio of the average level spacing to the cutoff value of the spacing, which is set by the resolution. The difference between the two kinds of distribution is easily discernible at the resolution of the experiments. As Figure 5 shows, the level spacing distribution is well described by a Wigner-type distribution. Thus, SEP appears to be sampling a regime of ergodic behavior in the 27900 cm^{-1} energy region on a time scale given by the average density of states. This time scale, $\sim$100 ps, is an approximate limit of the time on which ergodic vs regular behavior can be established within the limitations of the uncertainty principle. The only quantum numbers that remain defined are $l'' = 0$ and the rigorously good quantum numbers of J'' and parity. All other quantum numbers apparently lose their validity and cannot be used for labeling a state.

Even though the nearest neighbor spacings provide a quantum test of sorts for ergodicity, one can also approach this question from a more classical point of view. Here, the focus is on flows in phase space and the fraction of the phase space, made accessible by the preparation, that is actually sampled by molecular motion. Sundberg & Heller (43) have suggested that the measured spectral intensities contain the information on how much of the available phase space is being sampled. In considering

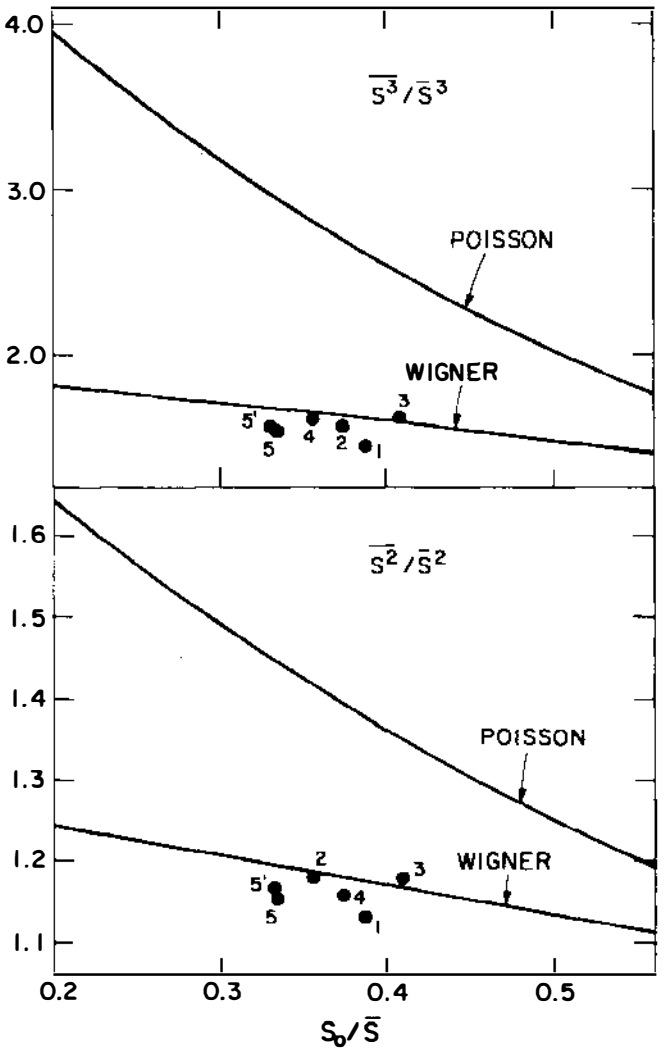

Figure 5 Second and third moments of nearest neighbor spacing distributions. The *dots* indicate values determined for six different clumps, and the *solid lines* show the Poisson and Wigner predictions. The theoretical curves are calculated for truncated Poisson and Wigner statistics, where the lower limit of the level spacings is equated with the linewidth of the DUMP laser.

the clumps observed in the acetylene SEP spectrum, the spectrum of each clump can be approximated as a summation of δ-functions

$$I_a(\omega) = \sum_n P_n^a \delta(\omega - E_n/\hbar) \qquad 3.$$

where a labels a particular clump, n indexes the eigenstates within the clump and P_n^a is the spectral intensity of a given line normalized so that the sum of spectral intensities is unity. Now, one can imagine a coherent excitation of the group of eigenstates $|n\rangle$ in the ath clump such that a nonstationary state $|a\rangle$ is prepared. It can be shown that the time averaged probability of a molecule starting in $|a\rangle$ and later being found in $|a\rangle$ is just the sum of the squares of the spectral intensities

$$P(a|a) = \lim_{T\to\infty} (1/T) \int_0^T \langle a|a(t)\rangle \, \mathrm{d}t = \sum_n (P_n^a)^2. \qquad 4.$$

As a result, $P(a|a)$ is inversely proportional to the number of phase space cells visited by the molecular motion. Although it looks from Eq. 4 as though this is an infinite-time measure, $P(a|a)$ will settle down to a stable value at a finite time T that is on the order of the reciprocal of the average level spacing within the clump.

In order to determine the fraction of available phase space that the motion samples, one needs to compare $P(a|a)$ evaluated from a spectrum with $P^{\mathrm{STO}}(a|a)$, the expected value of $P(a|a)$ when all of the available phase space is sampled stochastically. This raises the question of how $P^{\mathrm{STO}}(a|a)$ is to be evaluated. The method adopted in Ref. (37) makes use of Fourier transform techniques to obtain a frequency-smoothed envelope of the observed clump. The magnitude of the envelope at the position of the nth eigenstate is taken to be the value of the spectral intensity, $P_n^{a(\mathrm{STO})}$, and these expected intensities are then used to evaluate $P^{\mathrm{STO}}(a|a)$. That is, the smoothed envelope is assumed to represent the spread in energy corresponding to the preparation of a given clump. The observed individual transitions, whose intensities may deviate locally from that of the envelope, are assumed to appear at *every* energy eigenvalue within the clump.

The results of this intensity analysis on the six clumps indicate that 70–80% of the available phase space is sampled by the molecular motion in the high energy region under study. This is certainly in keeping with the earlier conclusion that ergodic behavior characterizes the molecular dynamics in this region. However, in interpreting the phase space test, some caution should be exercised because of the test's reliance on spectral intensities. Implementation of the $P(a|a)$ criterion for experimental data reveals difficulties, which were not apparent in earlier work based on calculated eigenvalues and intensities. The dynamic range of any measure-

ment is small compared to that possible in computations. In particular, SEP intensities can be measured only over a dynamic range of perhaps 50. Hence, there is always the possibility that weak transitions are missed. Weak features that are missed would have little effect on the calculation of $P(a|a)$, but they could have a significant effect on the calculation of $P(a|a)^{STO}$, since one is essentially assuming that the observed density of transitions corresponds to the correct density of states. In computation, one knows where all the level positions are and knows the local density of states precisely. For a real molecule, this local density can only be estimated, either from the observed density of transitions or by some method based on a Dunham expansion. In the 27900 cm^{-1} region of acetylene, the number of observed transitions exceeds that predicted from the Dunham calculation for a single l''-value by about a factor of three. In light of this problem, it is our feeling that the statistical properties of energy level spacings are more robust indicators of quantum ergodicity.

A second molecule that is currently being tested for quantum ergodicity is HCN. In the HCN experiment, the bent $\tilde{A}\ ^1A''$ electronic state ($\sim$52000 cm^{-1}) (23, 44), which is excited via a π^*–π transition, serves as the intermediate state; thus, the DUMP step produces substantial amounts of bending and CN stretching excitation. Since HCN has only one degenerate bending vibration instead of two as in acetylene, it provides a crucial test case for determining the role of bending excitation in bringing about ergodicity. A particularly interesting energy region to investigate is that where HCN is able to isomerize to HNC; the barrier to isomerization is approximately 17000 cm^{-1} (45, 46a–d). Classical trajectory studies by Lehmann, Scherer & Klemperer (47–50) indicate that chaotic motion ought to set in near this isomerization barrier. They did try to observe experimentally the onset of chaotic motion in HCN by exciting CH and CN stretch overtone transitions up to energies close to the isomerization barrier. However, they found, instead of signs of ergodicity, that the spectra are completely assignable and thus indicative of quasiperiodic motion.

An explanation for the difference between classical trajectory predictions and the quasiperiodic motion implied by the overtone spectra was suggested by Tennyson & Farantos (51). They claim that excitation of CH stretching overtones may correspond to observing quasiperiodic islands that are nested in a chaotic regime, and that it may be necessary to induce bending excitation in order to see chaotic motion. SEP is a technique well suited for sorting out what vibrational modes are important in bringing about chaotic motion and what kinds of initial preparations tend to keep energy localized. As we have shown, most of the SEP studies on these molecules have focused on the bending excitation. Yet, with a different

choice of the excited electronic state used in SEP, one could induce other types of vibrational excitation. For instance, if, in acetylene, the DUMP transitions originate from a linear excited state, the levels reached by the DUMP transition most likely will have a significant amount of C–C stretching excitation but very little bending motion. If the suggestion made by Tennyson & Farantos also applies to acetylene, then the new levels prepared by SEP through the linear intermediate state might correspond to quasiperiodic motion; the strong features in the SEP spectrum might be completely assignable, even at the high levels of excitation studied in the earlier acetylene experiments.

IVR in Formaldehyde as Studied by SEP

Many areas of reaction dynamics have relied on statistical models to provide adequate discriptions of chemical processes. A well-known example is the RRKM theory of unimolecular reactions. Closely related to these statistical pictures is the concept of IVR (52, 53), whereby vibrational energy that is initially placed in a certain vibrational mode eventually randomizes among all of the modes. To date, there have been numerous theoretical (17, 54–56) and experimental (52, 53) investigations of IVR. Generally, the focus is on the interactions responsible for IVR, the energy regimes in which the onset of IVR occurs, and the time scale over which energy randomization takes place. Fermi & Coriolis interactions are important mechanisms for bringing about IVR; however, control of these interactions in an experiment is often a very difficult matter. Earlier experimental work on excited aromatic compounds (52, 57), as well as the formaldehyde SEP (26) work, demonstrates the importance of Coriolis effects. Examples are sub-Doppler laser-induced fluorescence investigations of benzene (57), in which only $K_c = 0$ or $K_c = J$ levels are observed in the $14^1 1^2$ vibrational state of S_1, and molecular beam experiments on *p*-difluorobenzene (52), which show greater amounts of unstructured emission from specific energy regions of S_1 as the rotational temperature is increased. Unlike many earlier experiments, the SEP experiments on formaldehyde (26) take advantage of the combined rotational selection rules to bring about a clean preparation of different rotational levels within specific zeroth order vibrational states. Thus, the strength of the Coriolis interaction is systematically varied, and the rotational-state dependence of the Coriolis-induced vibrational mixing is explicitly shown.

In this work, $\tilde{X}$-state rotation-vibration levels between 7400–8600 cm^{-1} ($\rho_{vib} \sim 0.1$ per cm^{-1}) in the ground electronic state are probed by SEP. The observed levels fall into three distinct spectral features in this energy regime: a Fermi resonance between the $2_3 4_2$ and $1_1 2_1 3_2$ vibrational levels near 7460 cm^{-1}, the $2_4 4_4$ vibrational level near 8044 cm^{-1}, and the 2_5 and

$1_1 2_2 4_2$ vibrational levels near 8530 cm^{-1}. Figure 6 shows spectra of these features when different rotational components are reached; the asymmetric rotor states are indicated by the *labels* on each spectrum. It is immediately clear that, as the rotational excitation increases, more and more lines appear in the SEP spectrum. The density of lines is ~ 0.5 per cm^{-1} at the highest rotational levels that are excited. Observations here indicate that when $K_a = 0$, extra lines appear only for $J \geq 10$, while for

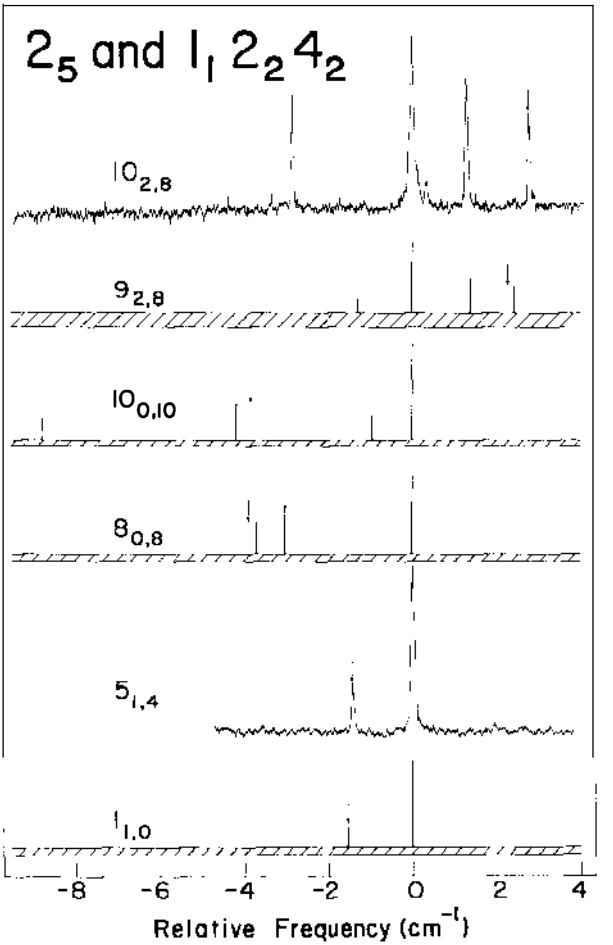

Figure 6 Rotational level dependence of SEP spectra near the $2_3 4_2$ and $1_1 2_1 3_2$ vibrational levels of formaldehyde (7460 cm^{-1}). The appearance of extra lines at high J, K_a values indicates vibrational mode mixing by Coriolis coupling. Mixing is substantial for $J \geq 10$ when $K_a = 0$, and $J \geq 6$ when $K_a = 1$ or 2.

$K_a = 1$ or 2, $J \geq 6$ is required before extra lines turn up in the spectrum. The extra lines that appear at higher J, K_a values arise from Coriolis-induced mixing of vibrational basis states in the $\tilde{X}$-state. As a result, the oscillator strength carried by a particular zeroth order state is shared among the rotation-vibration eigenstates of mixed character that result from the Coriolis interaction.

The observed state mixing is understood semiquantitatively by considering the symmetry rules and magnitudes of Coriolis interactions among the zeroth order rotation-vibration basis states (26). Here, Coriolis interaction is described in a basis in which the vibrational and rotational degrees of freedom are separated. The rotational selection rules and vibrational symmetry rules that describe which states are Coriolis coupled in formaldehyde (C_{2v} point group) are shown in Figures 7*a*,*b*, respectively; the *letters* labeling the *arrows* refer to the principal inertial axes about which the Coriolis coupling takes place. Coriolis effects couple vibrational states of different symmetry, so pure vibrational symmetry labels are destroyed; only the total rotation-vibration symmetry and the total angular momentum are preserved. The *a*, *b*, and *c* axis selection rules ($\Delta K_a = 0$, $\Delta K_c = \pm 1$; $\Delta K_a = \pm 1$, $\Delta K_c = \pm 1$; $\Delta K_a = \pm 1$, $\Delta K_c = 0$) also connect rotation-vibration levels with different values of the angular momentum projection onto the molecular axes. As a result, the projection quantum numbers K_a and K_c lose their validity.

Calculation of the Coriolis matrix elements themselves is simplified by the fact that formaldehyde is a near-prolate symmetric top ($\kappa = -0.9610$ for $v = 0$). Thus, the Coriolis matrix elements have nearly the same functional dependence that they would have in the prolate symmetric rotor limit, namely *a*-axis matrix elements are approximately proportional to K_a and the *b*,*c*-axis elements are approximately proportional to $J - K_a$. The Coriolis coupling matrix elements for H_2CO are calculated in a harmonic normal mode basis. Normal mode levels calculated to be within 60 cm^{-1} of the spectroscopically active level are considered for *b*,*c*-axis Coriolis mixing and levels as far away as 120 cm^{-1} are considered for *a*-axis mixing. Model spectra are then obtained from matrix diagonalization. The idea of these calculations is not to model accurately the details of the actual spectrum, but to compare the number of lines and the distribution of transition intensities to those of the observed spectrum (26).

The model spectra show the correct trend in that extra lines are predicted for increasing rotational excitation. Also, effects specific to the energy regions investigated in formaldehyde are reproduced. Specifically, the calculations indicate that no state will effectively couple to the 2_5 state. This result is borne out in the SEP spectra in the 8530 cm^{-1} region, where there is consistently a single line assignable to the 2_5 state regardless of the

amount of rotational excitation. The ν_2 mode corresponds to the C–O stretch, which is motion parallel to the *a*-axis; thus, *a*-axis coupling is not expected to be significant. Also, on the fairly simple grounds that the *b*- and *c*-rotational axes pass nearly through the center of the C=O bond (the only other masses in this molecule are the two light hydrogen atoms), the C–O stretch is not expected to be significantly affected by *b*,*c*-axis rotations

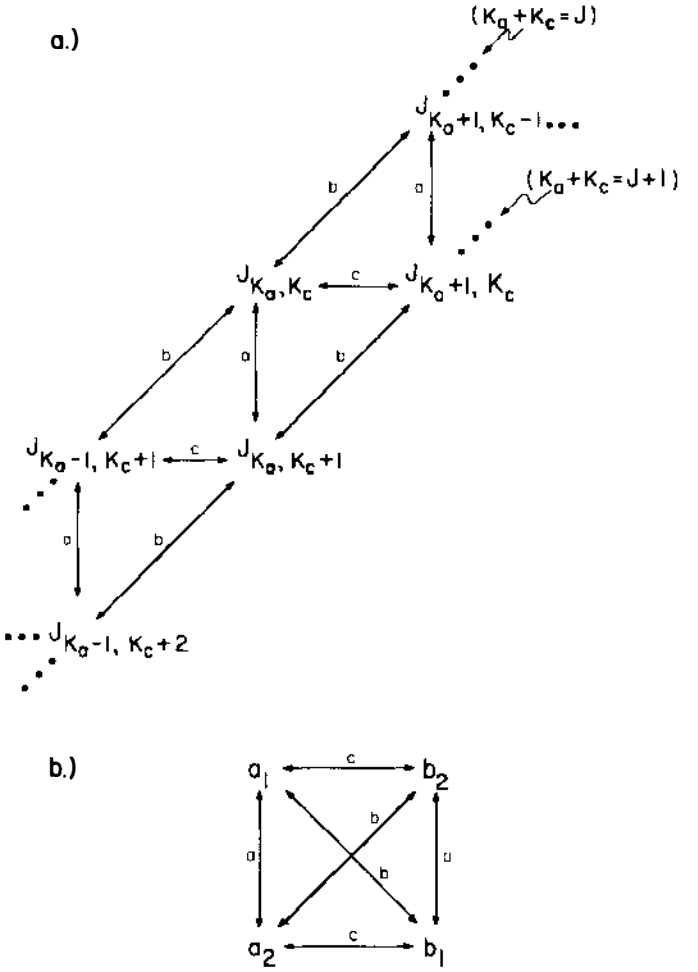

Figure 7 (*a*) Rotational selection rules for first-order Coriolis coupling. The *letters* above the arrows label the inertial axis about which the Coriolis interaction takes place. (*b*) Vibrational symmetry rules for Coriolis interactions. These vibrational rules apply to molecules with C_{2v} symmetry only. In this case, Coriolis interactions mix states of different vibrational symmetry.

either. Further support to the calculated spectra is given by predicted effects of the K_a quantum number. As an example, the $10_{0,10}$ level of the 2_34_2–$1_12_13_2$ combination is predicted to have no a-axis Coriolis coupling and b,c-axis matrix elements are expected to be small. Thus, intensity sharing should be negligible, with no extra lines appearing in the $10_{0,10}$ spectrum. For the $2_{2,0}$ level, where $K_a = 2$, the matrix elements are large for a-axis Coriolis interactions. However, within a 45 cm^{-1} interval containing the $2_{2,0}$ level, there are only three symmetry-allowed levels that can mix with the $2_{2,0}$ level. As a result, the model spectra predict that Coriolis interactions will produce no extra lines in this case either. These predictions for both the $10_{0,10}$ and $2_{2,0}$ level are confirmed in the observed spectra.

Even though the calculation in a harmonic normal mode basis is successful in predicting extra lines in regions where extra lines are observed, the calculated spectra always fall short of the number of lines actually observed. The harmonic normal mode picture has several defects. Firstly, when $K_a \neq 0$, there may be a strong a-axis Coriolis effect whereby states that are closely spaced can interact indirectly with each other through a distant intermediate state. For instance, the $1_12_26_1$ level interacts with the 2_34_2 level through the $2_34_16_1$ level (120 cm^{-1} away from $1_12_26_1$). The $2_34_16_1$ level is weakly coupled to the $1_12_26_1$ level but has a strong a-axis coupling to 2_34_2; thus, the $1_12_26_1$ level may borrow intensity from the 2_34_2 level. Secondly, treating the vibrations as though they were harmonic is certainly inappropriate. Cubic and quartic terms in the potential will anharmonically couple different harmonic oscillator states (Fermi coupling), to result in intensity-sharing apart from that caused by Coriolis effects. Finally, higher order Coriolis effects will relax the ΔK_a, ΔK_c selection rules and cause more extensive intensity sharing than would otherwise be predicted.

The SEP and model spectra demonstrate the importance of Coriolis coupling in mixing the vibrational states. As stated at the beginning of this section, Coriolis interactions are an important mechanism for bringing about IVR. In a recent classical mechanical study on vibrational energy flow, Coriolis interactions are considered as the primary mechanism by which energy flows between anharmonic normal modes (stretch and bend) of a triatomic molecule (58). The problem is formulated in terms of a hindered rotor model, according to which the effective kinetic energy of the rotor is proportional to the energy difference between the coupled vibrational modes, and the barrier height of the hindered rotation scales linearly with the angular momentum of the real rotating molecule. Energy transfer between the modes was found to be essentially complete as long as the kinetic energy of the hindered rotor is well below the barrier height. In other words, large rotational excitation of the molecule and a small

energy disparity between the coupled modes (but not zero) facilitate energy transfer. However, a small rotational excitation and a large energy disparity (kinetic energy > barrier height) inhibit transfer. These results qualitatively compare well with the SEP work on H_2CO and other experiments that show extensive vibrational mixing with increasing rotational quantum numbers. The classical model also lends support to the idea that distant vibrational states do not effectively couple by Coriolis interactions.

These conclusions lift Coriolis coupling from the realm of an obscure effect of interest only to high resolution spectroscopists, to an interaction likely to have practical consequences in several areas of chemistry. For instance, unimolecular reaction rates and multiphoton excitation depend strongly on densities of states, so proper methods of evaluating state densities must be known. The formaldehyde molecule itself provides an excellent example of how the inclusion of rotational effects in statistical rate theories (e.g. RRKM) can dramatically affect the predicted outcome of a dissociation process. Extensive photochemistry studies on formaldehyde (59) have shown that formaldehyde dissociates to either H_2+CO or $H+HCO$ upon excitation of the S_1 ($\tilde{A}\ ^1A_2$) excited electronic state. A likely dissociation route is via an internal conversion to S_0 with subsequent dissociation to products. Troe (60) has shed some light on this process by modeling the unimolecular breakup of S_0 into both product channels. He uses RRKM theory to describe the H_2+CO product channel and a statistical adiabatic method for modeling the $H+HCO$ channel. In both models, rotations are included in the state-counting procedure and an explicit J dependence of the dissociation rate constants is determined for each product channel. Among some of the effects observed are an increase in the dissociation threshold energies with increasing J and, more importantly, a switch in the dominant product channel (from H_2+CO to $H+HCO$) with increasing J. Thus, rotations dramatically affect the outcome of this dissociation.

Similar to unimolecular processes, multiphoton excitation is critically dependent on state densities. In multiphoton excitation, one is concerned primarily with an energy regime where the density of states is sufficiently high that a quasicontinuum sets in. In this regime, multiphoton excitation is a facile process, since each excitation step is essentially resonant. It is in the lower energy regime that multiphoton excitation runs into difficulty, since the molecule must possess enough resonant transitions to make the quasicontinuum accessible. The effect of increasing rotational excitation is to raise the density of states, thus shifting the quasicontinuum to lower energy regimes. The shift correspondingly makes multiphoton excitation more efficient, since fewer resonant transitions in low energy regions are required to reach the quasicontinuum (61).

Finally, Coriolis coupling adversely affects the prospects for mode specific chemistry. The first, and perhaps most obvious, way to avoid Coriolis effects is to excite rotationally cold states. However, even in the presence of rotational excitation, possibilities for mode specific chemistry remain promising as long as a judicious choice is made of which particular vibrational modes to excite. For instance, if one wants to excite a local stretching mode, the stretch coordinate needs to be aligned with the axis of rotation of the molecule in order to maintain mode purity. One can imagine inducing a stretch excitation along the top axis of a symmetric top molecule. Provided that $K \simeq J$ states are accessed in the excitation process, the stretch coordinate will be approximately parallel to the angular momentum vector, and Coriolis coupling of this stretching motion with other modes will be small. With regard to formaldehyde, the SEP work has shown that the 2_5 vibrational level does not appreciably Coriolis-couple to any other states. This is by virtue of vanishing a-axis matrix elements and negligibly small b,c-axis matrix elements. Thus, if one were to attempt mode selective chemistry on formaldehyde, ν_2 may be the appropriate mode to excite.

SEP PUMP-PROBE Techniques

In all of the work described so far, SEP is used solely as a spectroscopic tool for identifying states. However, SEP can also serve as an effective means of preparing a state, the evolution of which can then be monitored with a third PROBE laser. In a series of earlier experiments, Lawrance & Knight utilized this PUMP-DUMP-PROBE technique to measure collisional relaxation rates of excited vibrational levels in *p*-difluorobenzene (*p*DFB) (62, 63). The main motivation for their studies stemmed from an apparent disparity of vibrational relaxation rates in ground and excited electronic states. Relaxation of excited vibrational levels within the ground state manifold is known to require anywhere from tens to thousands of collisions (64). Yet, vibrational levels of some electronically excited aromatic compounds relax at rates that are often in excess of the gas kinetic rate (65). This has raised the question of whether the huge difference in relaxation rates is due to some particular property of the excited electronic state or if it is simply a characteristic of the class of molecules undergoing relaxation.

With the ability of SEP to reach high-lying vibrational levels in the ground state manifold, the question of whether an excited electronic state possesses some peculiar property can be addressed. In the experiments on *p*DFB, SEP is used to prepare the molecules in the $5_2 30_2$ vibrational level; the PUMP and DUMP transitions are the $5_0^1 30_2^2$ and $5_2^1 30_2^2$ bands of the $S_1(^1B_{2u})$–$S_0(^1A_g)$ system, respectively. Following preparation of the $5_2 30_2$

level, the population of this level is measured at delays of 80–300 ns after the DUMP pulse by a PROBE laser tuned to the $5_2^0 30_2^2$ transition. The detected signal is the single vibronic level fluorescence (SVLF) induced by the PROBE. The only reason delay times shorter than 80 ns are not used is to assure rotational equilibration prior to probing the SEP-prepared level.

Deactivation rates of the $5_2 30_2$ level are measured for collision partners ranging from very light gases such as helium and H_2 to heavier molecules such as *p*DFB itself and various isomeric forms of pentanol. In all cases, the decay is observed to be a single exponential. The deactivation rate constants, which are extracted from the decays, span a wide range of values, from a minimum of 0.76×10^7 Torr^{-1} s^{-1} for helium to a maximum of 4.1×10^7 Torr^{-1} s^{-1} for diethyl ether. The corresponding deactivation cross sections are 18 Å^2 and 339 Å^2, respectively. Of the 23 collision partners for which measurements were made, 20 of them deactivate the $5_2 30_2$ state at a rate exceeding the hard sphere collision rate ($(1–2) \times \sigma_{HS}$). The only gases for which the deactivation rate is less than the hard sphere rate are He, H_2, and D_2, the lightest collision partners. Approximately 4, 2, and 1.5 collisions are required for deactivation with these three gases, respectively.

That most of the deactivation rates exceed the hard sphere collision rate should not be too surprising. The hard sphere picture does not really describe the intermolecular forces that affect a collision. A model that more adequately predicts the deactivation rates is one in which a Lennard-Jones potential is used to describe the interaction between the collision pair (63). The success of the Lennard-Jones model for most collision partners suggests that the attractive part of the Lennard-Jones potential gives rise to the large deactivation rate constants that are observed, and that the relaxation process is quite insensitive to any internal structure in *p*DFB or its collision partner. The Lennard-Jones model is seriously inadequate only for He, H_2, and D_2. Deactivation by He, H_2, or D_2 is likely to differ from deactivation by a heavier gas in that there is a difference in the number of pathways or channels for relaxation. Thus, it is entirely possible that the anomalous behavior of the three lighter gases may arise from a restriction of the number of relaxation channels as well as from unfavorable momentum gaps that may result from such a restriction.

SEP pump-probe techniques have been extended to measurements of rotational relaxation rates as well (66). As part of the study on *p*DFB, the rate of rotational relaxation within the $5_2 30_2$ state caused by *p*DFB–*p*DFB collisions is measured as a function of the *p*DFB pressure. In this measurement, the laser bandwidths are not sufficiently narrow to populate a single rotational level by SEP; rather, a group of 200–300 $|J'', K''\rangle$ levels

are prepared. Nevertheless, the decay of the group of states is still expected to follow pseudo-first-order kinetics. The decay rate constant asymptotically approaches the vibrational relaxation rate as the *p*DFB pressure is raised, thus allowing one to extract the rate constant for rotational relaxation from decays measured over a wide pressure range. The results indicate that rotational relaxation is also an extremely efficient process. In pure *p*DFB, the measured rate constant for rotational relaxation is observed to be five times the hard sphere value.

In recent studies of rotation relaxation in formaldehyde, the newly developed technique of Transient Absorption Polarization Spectroscopy (TAPS) (2) is used to measure the decay rate of an SEP prepared state. The TAPS technique is unusual in that it measures the decay of a state through the decay in a rotated polarization of a cw probe beam. The technique relies on SEP to be not only able to populate a certain rotation-vibration level, but also to populate that level with a specific alignment in the laboratory frame. The advantage of the TAPS technique is that the polarization rotation that one detects is present *only* if the SEP prepared level is populated. In the language of molecular beam resonance, it is a "flop in" rather than a "flop out" measurement. Thus, TAPS eliminates the large background levels that plague other techniques, such as transient absorption spectroscopy. This is an extremely important factor in the TAPS PUMP-DUMP-PROBE experiments on H_2CO, since the cw dye laser probing the states has amplitude noise that is large enough in the frequency region of our kinetic decay rates to prohibit a transient *absorption* measurement.

As an example of how the TAPS method works, PUMP and DUMP pulses with vertical polarizations are tuned to populate the $4_{1,3}$ asymmetric rotor level of the $2_4 4_4$ vibrational state ($\varepsilon_{vib} = 11400\ cm^{-1}$); the PUMP and DUMP transitions are $4_0^3 {}^pQ_1[4]$ and $2_4^0 4^3 4^pQ_1[4]$, respectively. Thus, the $2_4 4_4\ 4_{1,3}$ vibrational-rotation level is populated with a definite alignment. A cw laser with its polarization inclined at 45° with respect to the PUMP and DUMP polarizations is tuned onto the $2_4^0 4_4^1 {}^pQ_1[4]$ transition to probe the SEP prepared level. Since the $2_4 4_4\ 4_{1,3}$ level is aligned, the polarization components of the probe laser that are parallel and perpendicular to the prepared alignment will have slightly different absorptivities. As a result, the amplitude of one component becomes diminished relative to the other, thus causing the polarization of the probe laser to rotate. As the population in the $2_4 4_4\ 4_{1,3}$ level is depleted, the components approach equal magnitude again and the polarization rotates back to its original 45° position.

A signal is measured by placing a polarization filter in the path of the cw PROBE laser and detecting any cw laser light that is passed by the

filter. The filter blocks all of the cw beam when its polarization is at 45°. However, some of the cw PROBE beam leaks through the filter if the cw polarization is rotated; the light that leaks through is subsequently detected with a photomultiplier. This method of detection is quite sensitive, since one obtains the complete temporal information of the prepared level on each SEP pulse sequence and signal averaging techniques can be used to greatly enhance the signal-to-noise ratio. A signal-to-noise ratio of approximately 1000 after 1000 shots is not uncommon. It should be noted that the difference in the electric field components of the PROBE beam, which gives rise to the optical rotation, is linearly dependent on the population of the aligned state. What is observed is the square amplitude of the component orthogonal to the 45° polarization. Since it is the square amplitude that is detected, the decay rate of the optical rotation will be intrinsically twice the decay rate of the *population* of the probe state.

Rates of deactivation of several rotation-vibration levels by formaldehyde-formaldehyde collisions have been measured with this technique. The SEP prepared states are all in the energy range of 11000–12000 cm^{-1}. The deactivation rate constants that are extracted from a Stern-Volmer analysis (over a pressure range of 0–200 mTorr) all have values of approximately 250 μs^{-1} $Torr^{-1}$, a value that is approximately an order of magnitude larger than the rate constant for hard sphere collisions. Again, this result is not too surprising in light of the fact that the relaxation process is controlled mainly by long-range dipole-dipole attractions (67), which result from the large permanent dipole moment of ground state formaldehyde (2.33 D) (11).

Even though the total deactivation rates may show no interesting variations from one vibrational state to the next, the individual state-to-state cross sections for the relaxation channels may display propensities characteristic of specific inter- and intramolecular processes. In a quasi-periodic regime, states that are near each other in energy are well separate in vibrational quantum number space. Hence, one expects strong vibrational propensity rules for relaxing to neighboring states in a given energy region to exhibit strikingly different state-to-state cross sections. In an ergodic regime, however, all states in a small energy regime are expected to sample exactly the same regions of phase space. Accordingly, the state-to-state cross sections are expected to show very little variation between different initial or different final states. No strong propensity rules will apply in this case.

In order to gain state-to-state rate information, the TAPS technique is currently being extended to probe target levels that are likely to receive population *from* the SEP prepared level. In pure formaldehyde, rotational relaxation is expected to obey *a*-axis electric dipole section rules ($\Delta J = \pm 1$,

$\Delta K_a = 0$) (67–69). In a preliminary state-to-state measurement, the $2_4 4_4$ $4_{1,3}$ level is prepared by SEP and the time evolution of the $2_4 4_4$ $5_{1,4}$ target level is monitored by the TAPS technique. The $5_{1,4}$ level is observed to rise and fall, with the rise time of the $5_{1,4}$ level matching the decay time of the $4_{1,3}$ level. It is important to realize that the success of the TAPS method in state-to-state measurements depends on preserving the alignment generated by SEP as the population is transferred out of the prepared level into the target levels. Alignment preservation is expected and is observed not only in the above TAPS measurement, but also in independent state-to-state measurements in several other molecules (70–72). Also, as we have noted, a TAPS signal scales with the square of the population in the level being probed. While the TAPS signal on the level initially prepared by SEP may be large, collisions could spread the population of that level over a large number of target levels. Then, the TAPS method may not have the sensitivity to enable a precise state-to-state measurement. In that case, a probe technique such as single vibronic level fluorescence may be more suitable.

SUMMARY

We have discussed in some detail the SEP technique and how it is applied in several areas of spectroscopy and molecular dynamics. What makes this technique so versatile is its ability to simplify spectra, through combined selection rules, and to interrogate a wider range of internal molecular energies. SEP has been very fruitful in yielding such fundamental quantities as extended Dunham coefficients and rate constants for deactivation, and it has provided valuable insights into more abstract concepts, such as quantum ergodicity. Many of the experimental investigations discussed are in their infancy. Undoubtedly, as SEP experiments become more refined, they will begin to address more advanced questions, such as what particular regions of phase space tend to keep energy localized, and whether or not there exist specific molecular preparations that will promote a certain type of photochemical process. Eventually, as the sensitivity of SEP improves, many of the same investigations that are done on stable molecules can be done on highly reactive intermediates. Spectroscopic characterization as well as measurement of dynamical processes involving these intermediates would be of immense value in areas such as combustion or atmospheric chemistry. Finally, it is conceivable that SEP or some variant of it could move into the realm of ultrafast dynamics, whereby SEP induces and monitors rapid processes such as a photodissociation event.

ACKNOWLEDGMENTS

This work was supported in part by a contract from the Department of Energy (DE-AC02-81ER10831) and in part by a grant from the Air Force Office of Scientific Research (AFOSR-85-0381).

Literature Cited

1. Vaccaro, P. H., Redington, R. L., Schmidt, J., Kinsey, J. L., Field, R. W. 1985. *J. Chem. Phys.* 82: 5755
2. Vaccaro, P. H., Temps, F., Kinsey, J. L., Field, R. W. 1986. Work in progress
3. Weickenmeyer, W., Diemer, U., Wahl, M., Raab, M., Demtröder, W., Müller, W. 1985. *J. Chem. Phys.* 82: 5354
4. Cooper, D. E., Klimcak, C. M., Wessel, J. E. 1981. *Phys. Rev. Lett.* 46: 324
5. DePristo, A. E., Rabitz, H., Miles, R. B. 1980. *J. Chem. Phys.* 73: 4798
6. Esherick, P., Owyoung, A. 1982. *Adv. Infrared Raman Spectrosc.* 9: 130–87
7. Esherick, P., Owyoung, A., Pliva, J. 1985. *J. Chem. Phys.* 83: 3311
8. Crim, F. F. 1984. *Ann. Rev. Phys. Chem.* 35: 657
9. King, D. S. 1982. *Adv. Chem. Phys.* 50: 105
10. Reisner, D. E., Field, R. W., Kinsey, J. L., Dai, H. L. 1984. *J. Chem. Phys.* 80: 5984
11. Vaccaro, P. H., Kinsey, J. L., Field, R. W., Dai, H. L. 1983. *J. Chem. Phys.* 78: 3659
12. Reddy, K. V., Heller, D. F., Berry, M. J. 1982. *J. Chem. Phys.* 76: 2814
13. Rizzo, T. R., Hayden, C. C., Crim, F. F. 1984. *J. Chem. Phys.* 81: 4501
14. Heller, E. J. 1983. *Faraday Discuss. Chem. Soc.* 75: 141
15. Marcus, R. A. 1983. *Faraday Discuss. Chem. Soc.* 75: 103
16. Noid, D. W., Koszykowski, M. L., Marcus, R. A. 1981. *Ann. Rev. Phys. Chem.* 32: 267
17. Rice, S. A. 1981. *Adv. Chem. Phys.* 47: 117
18. Percival, I. C. 1973. *J. Phys. B* 6: L229
19. Reinhardt, W. P. 1982. *J. Phys. Chem.* 86: 2158
20. Percival, I. C. 1977. *Adv. Chem. Phys.* 36: 1
21. Shirts, R. B., Reinhardt, W. P. 1982. *J. Chem. Phys.* 77: 5204
22. Shirts, R. B., Reinhardt, W. P. 1983. *J. Chem. Phys.* 79: 3173
23. Herzberg, G. 1966. *Electronic Spectra of Polyatomic Molecules.* New York: Van Nostrand Reinhold
24. Moll, D. J., Parker, G. R. Jr., Kuppermann, A. 1984. *J. Chem. Phys.* 80: 4800
25. Nakagawa, T., Kashiwagi, H., Kurihara, H., Moriono, Y. 1969. *J. Mol. Spectrosc.* 31: 436
26. Dai, H. L., Korpa, C. L., Kinsey, J. L., Field, R. W. 1985. *J. Chem. Phys.* 82: 1688
27. Gerber, R. B., Roth, R. M., Ratner, M. A. 1981. *Mol. Phys.* 44: 1335
28. Handy, N. C., Carter, S. 1981. *Chem. Phys. Lett.* 79: 118
29. Maessen, B., Wolfsberg, M. 1984. *J. Chem. Phys.* 80: 4651
30. Bunker, P. R. 1979. *Molecular Symmetry and Spectroscopy.* New York: Academic Press
31. Romanowski, H., Bowman, J. M., Harding, L. B. 1985. *J. Chem. Phys.* 82: 4155
32. Harding, L. B., Ermler, W. C. 1985. *J. Comput. Chem.* 6: 13
33. Tobin, F. L., Bowman, J. M. 1980. *Chem. Phys.* 47: 151
34. Christoffel, K. M., Bowman, J. M. 1982. *Chem. Phys. Lett.* 85: 220
35. Abramson, E., Field, R. W., Imre, D., Innes, K. K., Kinsey, J. L. 1984. *J. Chem. Phys.* 80: 2298
36. Abramson, E., Field, R. W., Imre, D., Innes, K. K., Kinsey, J. L. 1985. *J. Chem. Phys.* 83: 453
37. Sundberg, R. L., Abramson, E., Kinsey, J. L., Field, R. W. 1985. *J. Chem. Phys.* 83: 466
38. Skodje, R. T., Borondo, F., Reinhardt, W. P. 1985. *J. Chem. Phys.* 82: 4611
39. Deleon, N., Davis, M. J., Heller, E. J. 1984. *J. Chem. Phys.* 80: 794
40. Berry, M. V., Tabor, M. 1977. *Proc. R. Soc. London Ser. A* 356: 375
41. Wigner, E. P. 1967. *SIAM Rev.* 9: 1
42. Brody, T. A., Flores, J., French, J. B., Mello, P. A., Pandey, A., Wong, S. S. M. 1981. *Rev. Mod. Phys.* 53: 385
43. Sundberg, R. L., Heller, E. J. 1985. In *Chaotic Behavior in Quantum Systems*, ed. G. Casati. New York: Plenum
44. Herzberg, G., Innes, K. K. 1957. *Can. J. Phys.* 35: 842

45. Ross, S. C., Bunker, P. R. 1983. *J. Mol. Spectrosc.* 101: 199
46a. Carter, S., Mills, I. M., Murrell, J. N. 1980. *J. Mol. Spectrosc.* 81: 110
46b. Pearson, P. R., Schaefer, H. F. III, Wahlgren, U. 1975. *J. Chem. Phys.* 62: 350
46c. Perić, M., Mladenovic, M., Peyerimhoff, S. D., Buenker, R. J. 1983. *Chem. Phys.* 82: 317
46d. Murrell, J. N., Carter, S., Halonen, L. O. 1982. *J. Mol. Spectrosc.* 93: 307
47. Lehmann, K. K., Scherer, G. J., Klemperer, W. 1982. *J. Chem. Phys.* 76: 6441
48. Lehmann, K. K., Scherer, G. J., Klemperer, W. 1982. *J. Chem. Phys.* 77: 2853
49. Lehmann, K. K., Scherer, G. J., Klemperer, W. 1983. *J. Chem. Phys.* 78: 608
50. Farrelly, D., Reinhardt, W. P. 1983. *J. Chem. Phys.* 78: 606
51. Tennyson, J., Farantos, S. C. 1985. *Chem. Phys.* 93: 237
52. Parmenter, C. S. 1983. *Faraday Discuss. Chem. Soc.* 75: 7
53. Smalley, R. E. 1982. *J. Phys. Chem.* 86: 3504
54. Sibert, E. L. III, Reinhardt, W. P., Hynes, J. T. 1984. *J. Chem. Phys.* 81: 1115
55. Sibert, E. L. III, Hynes, J. T., Reinhardt, W. P. 1984. *J. Chem. Phys.* 81: 1135
56. Hutchinson, J. S., Reinhardt, W. P., Hynes, J. T. 1983. *J. Chem. Phys.* 79: 4247
57. Riedle, E., Neusser, H. J., Schlag, E. W. 1982. *J. Phys. Chem.* 86: 4847
58. Uzer, T., Natanson, G. A., Hynes, J. T. 1985. *Chem. Phys. Lett.* 122: 12
59. Moore, C. B., Weisshaar, J. C. 1983. *Ann. Rev. Phys. Chem.* 34: 525
60. Troe, J. 1984. *J. Phys. Chem.* 88: 4375
61. Bassi, D., Boschetti, A., Scoles, G., Scotoni, M., Zen, M. 1982. *Chem. Phys.* 71: 239
62. Lawrance, W. D., Knight, A. E. W. 1982. *J. Chem. Phys.* 77: 570
63. Lawrance, W. D., Knight, A. E. W. 1983. *J. Chem. Phys.* 79: 6030
64. Lambert, J. D. 1977. *Vibrational and Rotational Relaxation in Gases.* Oxford: Clarendon
65. Parmenter, C. S. 1982. *J. Phys. Chem.* 86: 1735
66. Lawrance, W. D., Knight, A. E. W. 1983. *J. Phys. Chem.* 87: 389
67. Oka, T. 1973. *Adv. Atomic Molec. Phys.* 9: 127
68. Orr, B. J., Haub, J. G., Nutt, G. F., Steward, J. L., Vozzo, O. 1981. *Chem. Phys. Lett.* 78: 621
69. Orr, B. J., Haub, J. G., Haines, R. 1984. *Chem. Phys. Lett.* 107: 168
70. Brechignac, P. 1982. *J. Chem. Phys.* 76: 3389
71. Johns, J. W. C., McKellar, A. R. W., Oka, T., Romheld, M. 1975. *J. Chem. Phys.* 62: 1488
72. McCaffrey, A. J., Proctor, M. J., Whitaker, B. J. 1986. *Ann. Rev. Phys. Chem.* 37: 223–44